




^{99m}Tc-AgNPs-ICG: nanoparticle for hybrid image.

^{99m}Tc-AgNPs-ICG: nanopartícula para imagen híbrida

^{99m}Tc-AgNPs-ICG: nanopartícula para imagem híbrida.

 <https://doi.org/10.35954/SM2024.43.1.5.e302>


Stephanie Simois ^a  <https://orcid.org/0000-0003-0545-2180>


Agostina Cammarata ^b  <https://orcid.org/0000-0003-2828-5194>


Romina Glisoni ^c  <https://orcid.org/0000-0002-7845-1800>

Mirel Cabrera ^d  <https://orcid.org/0000-0002-5225-1106>

Marcos Tassano ^e  <https://orcid.org/0000-0001-6685-4656>

Juan Pablo Gambini ^f  <https://orcid.org/0000-0001-5368-3464>

Ximena Aida Camacho Damata ^g  <https://orcid.org/0000-0002-0755-3834>

Pablo Cabral ^h  <https://orcid.org/0000-0001-7344-2027>

(a,d,e,g,h) Universidad de la República, Facultad de Ciencias. Departamento de Radiofarmacia. Centro de Investigaciones Nucleares. Montevideo, Uruguay.

(b,c) Universidad de Buenos Aires, Facultad de Farmacia y Bioquímica. Departamento de Tecnología Farmacéutica, Instituto de Nanobiotecnología NANOBIOTEC (UBA-CONICET). Buenos Aires, Argentina.

(f) Universidad de la República, Facultad de Medicina. Hospital de Clínicas. Centro de Medicina Nuclear e Imagenología Molecular. Montevideo, Uruguay.

Citation this article / Cómo citar este artículo / Como citar este artigo

Simois S, Cammarata A, Glisoni R, Cabrera M, Tassano M, Gambini JP, *et al.* ^{99m}Tc-AgNPs-ICG: nanoparticle for hybrid image. *Salud Mil* [Internet]. 20 February 2024 [cited DD MM YYYY];43(1):e302. Available from: <https://revistasaludmilitar.uy/ojs/index.php/Rsm/article/view/421> DOI: 10.35954/SM2024.43.1.5.e302.

ABSTRACT

Introduction: Currently nanotechnology has radically changed the diagnosis of many human pathologies. The aim of this work is to obtain silver nanoparticles for hybrid imaging (^{99m}Tc-AgNPs-ICG) having potential clinical imaging applications.

Materials and methods: We mixed 2 ml of ascorbic acid (1.7 x 10⁻⁴ M), 5 mCi of ^{99m}TcO₄⁻, 2 ml of citric acid (8.0 x 10⁻⁴ M) and 0.5 ml of silver nitrate (2.5 x 10⁻³ M). Solution pH was 5, and it was shaken for 20 minutes at 37° C. Afterwards, 2 μL of Indocyanine Green (1.3 x 10⁻³ M) was added (^{99m}Tc-AgNPs-ICG). Physicochemical properties of the solution were characterized by UV (λ₁ = 420 nm, λ₂ = 254 nm) and gamma detector. Fluorescence image, particle size and IR spectrum were evaluated.

Results: Silver nanoparticles were obtained in aqueous solution a pH of 5. Their pH, color and spectrum were stable for seven days. Furthermore, the principal peak characterized by HPLC, UV and Gamma detector had similar retention times. Its UV spectrum showed an absorption band of 420 nm, which corresponds to the plasmon absorption band of these nanoparticles. The particle size was 46 nm ± 1.5 nm. The IR spectrum showed absorption bands in 3193, 2624, 1596 y 1212 cm⁻¹.

Received for review: November 2023.

Accepted for publication: February 2024.

Correspondence: Centro de Investigaciones Nucleares, Facultad de Ciencias, Universidad de la República, Montevideo, Uruguay. Mataojo 2055, P.O. 11400, Montevideo, Uruguay. Tel: (+5982) 5250901/108; fax: (+5982) 5250895.

Contact e-mail: pabloc7@gmail.com

Conclusions: We describe for the first time in literature the synthesis of hybrid (radioactive and fluorescent) silver nanoparticles. Their physiochemical properties were characterized, being stable and their labelling was reproducible having potential biomedical applications.

KEYWORDS: Silver Compounds; ^{99m}Tc-HID; Sodium Pertechnetate Tc 99m; Metal Nanoparticles; Indocyanine Green.

RESUMEN

Introducción: actualmente la nanotecnología ha cambiado radicalmente el diagnóstico de muchas patologías humanas. El objetivo de este trabajo es obtener nanopartículas de plata para imagen híbrida (^{99m}Tc-AgNPs-ICG) que tengan potenciales aplicaciones clínicas en imagen.

Materiales y métodos: se mezclaron 2 ml de ácido ascórbico (1.7×10^{-4} M), 5 mCi de ^{99m}TcO₄⁻, 2 ml de ácido cítrico (8.0×10^{-4} M) y 0.5 ml de nitrato de plata (2.5×10^{-3} M). El pH de la solución fue 5, y se agitó durante 20 minutos a 37° C. A continuación, se añadieron 2 µl de verde de indocianina (1.3×10^{-3} M) (^{99m}Tc-AgNPs-ICG). Las propiedades fisicoquímicas de la solución se caracterizaron mediante UV ($\lambda_1 = 420$ nm, $\lambda_2 = 254$ nm) y detector gamma. Se evaluaron la imagen de fluorescencia, el tamaño de las partículas y el espectro IR.

Resultados: se obtuvieron nanopartículas de plata en solución acuosa a un pH de 5. Su pH, color y espectro fueron estables durante siete días. Además, el pico principal caracterizado por HPLC, UV y detector Gamma tenía tiempos de retención similares. Su espectro UV mostró una banda de absorción de 420 nm, que corresponde a la banda de absorción plasmónica de estas nanopartículas. El tamaño de las partículas era de $46 \text{ nm} \pm 1,5 \text{ nm}$. El espectro IR mostró bandas de absorción en 3193, 2624, 1596 y 1212 cm^{-1} .

Conclusiones: describimos por primera vez en la literatura la síntesis de nanopartículas de plata híbridas (radioactivas y fluorescentes). Se caracterizaron sus propiedades fisicoquímicas, siendo estables y su etiquetado fue reproducible teniendo potenciales aplicaciones biomédicas.

PALABRAS CLAVE: Compuestos de Plata; Lidofenina de Tecnecio Tc 99m; Nanopartículas del Metal; Pertechnetato de Sodio Tc 99m; Verde de Indocianina.

RESUMO

Introdução: Atualmente, a nanotecnologia mudou radicalmente o diagnóstico de muitas patologias humanas. O objetivo deste trabalho é obter nanopartículas de prata para imagens híbridas (^{99m}Tc-AgNPs-ICG) com possíveis aplicações de imagens clínicas.

Materiais e métodos: Misturamos 2 ml de ácido ascórbico (1.7×10^{-4} M), 5 mCi de ^{99m}TcO₄⁻, 2 ml de ácido cítrico (8.0×10^{-4} M) e 0.5 ml de nitrato de prata (2.5×10^{-3} M). O pH da solução era 5 e ela foi agitada por 20 minutos a 37° C. Em seguida, foram adicionados 2 µL de indocianina verde ($1,3 \times 10^{-3}$ M) (^{99m}Tc-AgNPs-ICG). As propriedades físico-químicas da solução foram caracterizadas por UV ($\lambda_1 = 420$ nm, $\lambda_2 = 254$ nm) e detector gama. A imagem de fluorescência, o tamanho das partículas e o espectro de infravermelho foram avaliados.

Resultados: As nanopartículas de prata foram obtidas em solução aquosa com pH de 5. Seu pH, cor e espectro permaneceram estáveis por sete dias. Além disso, o pico principal caracterizado por HPLC, UV e detector gama teve tempos de retenção semelhantes. Seu espectro de UV mostrou uma banda



de absorção de 420 nm, que corresponde à banda de absorção plasmônica dessas nanopartículas. O tamanho da partícula foi de $46 \text{ nm} \pm 1,5 \text{ nm}$. O espectro de IV mostrou bandas de absorção em 3193, 2624, 1596 e 1212 cm^{-1} .

Conclusões: Descrevemos pela primeira vez na literatura a síntese de nanopartículas de prata híbridas (radioativas e fluorescentes). Suas propriedades físico-químicas foram caracterizadas, sendo estáveis e sua rotulagem foi reprodutível, com possíveis aplicações biomédicas.

PALAVRAS-CHAVE: Compostos de Prata; Lidofenina-99mTc; Nanopartículas Metálicas; Pertecnetato Tc 99m de Sódio; Verde de Indocianina.

INTRODUCTION

Silver, represented by Ag symbol, has been used for many years as a precious metal. This metal is characterized for both its brilliant color and some important properties; such as ductility and malleability. Since silver comes from the d block of the periodic table, it is a transition metal (group 11 and period 5). Its atomic mass corresponds to 107.8682, its density is 10.49 g/cm^3 , its melting point is 962° C , and finally 2162° C corresponds to its boiling point. Almost all of silver chemical compounds have an oxidation number of +1. Moreover, silver's antibacterial properties have been widely studied because the toxicity in human cells is considerably lower than to bacteria (1,2).

Nanotechnology has many definitions and applications. However, all definitions highlight the design and development of highly ordered bottom-up nanostructured materials that offer specific responses when exposed to certain stimuli (3,4).

In contemporary industrial contexts, metallic nanoparticles have gained substantial prominence, finding diverse applications across sectors such as electronics, biology, and medicine (5).

This growing prominence is attributed to the expanding significance of nanoscale chemical entities in recent decades, driven by their multifaceted and pioneering prospects. The inherent potential within metallic nanoparticles enables precise manipulation of parameters like shape, size, color, and surface characteristics, empowering researchers with control over their properties.

Silver nanoparticles (AgNPs) have been particularly studied in order to use them in biomedical applications, for instance, they have proved to have antibacterial properties (6-8).

Furthermore, there are a many chemical methods that describe the synthesis and characterization of nanoparticles. Providing that different reducing and stabilizing agents are used, AgNPs become soluble in aqueous solution showing powerful optical and biomedical properties (9,10).

Cancer represents a global health challenge, arising from a complex interplay of environmental factors and genetic mutations. These mutations trigger a cascade of molecular events at the cellular level, ultimately culminating in the formation of tumors. Persistent exposure to low levels of oxidative stress has been identified as a potential contributor to cancer initiation by evading apoptosis (11).

Numerous investigations have demonstrated the intracellular localization of AgNPs within the perinuclear space of the cytoplasm and endolysosomal compartments as they enter cells via endocytosis (12).

AgNPs disrupt cellular respiration and generate reactive oxygen species (ROS). This detrimental impact on cells leads to oxidative stress, DNA damage, apoptosis induction, and mitochondrial impairment in cancer cells (13-16).

The concept of theranostics, which amalgamates diagnostics and therapy, finds application in biosynthesized AgNPs due to their dual functionality. These AgNPs exhibit anti-cancer

properties and are employed in targeted drug delivery and bioimaging vehicles.

In medical imaging, nuclear imaging techniques emerge as indispensable tools, primarily including positron emission tomography (PET) and single photon emission computed tomography (SPECT). These techniques exhibit an exceptional capability to provide quantitative insights into biological phenomena *in vivo*. However, the clinical utility of these methods is tempered by their limitation of relatively low spatial resolution (17,18).

Conversely, fluorescent imaging stands as a compelling alternative with notably enhanced spatial resolution. Even more, indocyanine green (ICG), whose light-responsive attributes harness the precision of fluorescent imaging for real-time intraoperative delineation, resonating as an adept complement to nuclear imaging modalities. The aim of this work is to obtain silver nanoparticles for hybrid imaging (radioactive / fluorescent) (^{99m}Tc-AgNPs-ICG), with potential theranostic agent.

MATERIALS AND METHODS

The materials used were silver nitrate (99.9%, Sigma Aldrich), ascorbic acid (Sigma Aldrich), citric acid (May & Baker LTD Dagenham England), sodium hydroxide (Anedra), indocyanine green (ICG) (Hub Pharmaceuticals.), Generator ⁹⁹Mo/^{99m}Tc (Technonuclear).

1. Fluorescent silver nanoparticles synthesis (AgNPs-ICG)

We mixed 20 ml of ascorbic acid (1.7×10^{-4} M) with 20 ml of citric acid (8.0×10^{-4} M) and 5 ml of the silver nitrate solution (2.5×10^{-3} M), constantly shaking at 90 rpm and 37° C. Solution pH was modified to 6 using a solution of 0.1 M sodium hydroxide, and it was shaken for 20 minutes at a controlled temperature of 37° C. Then, 20 μ L of ICG (1.3×10^{-3} M) were added (AgNPs-ICG). The nanoparticles were evaluated by size molecular exclusion chromatography, using PD-10 Sephadex G25 (Cytiva), mobile fase 0.9% NaCl,

taken fractions of 1 mL. Subsequent to this, a UV-visible analysis spanning the spectral range of 200 to 700 nm was executed to discern spectral shifts and changes in the suspension's hue for a period of 7 days.

2. Labelling of AgNPs-ICG with ^{99m}Tc (^{99m}Tc-AgNPs-ICG)

The synthesis process commenced with the combination of 2 ml of ascorbic acid (1.7×10^{-4} M) and 5 mCi of ^{99m}TcO₄⁻. This mixture was integrated with 2 ml of citric acid (8.0×10^{-4} M) and then added 0.5 ml of a silver nitrate solution (2.5×10^{-3} M), ensuring continuous agitation throughout.

Adjusting the pH to 6 was achieved by introducing a 0.1 M solution of sodium hydroxide, followed by vigorous shaking for duration of 20 minutes at a controlled temperature of 37° C.

Subsequently, 2 μ L of ICG (1.3×10^{-3} M) were introduced, culminating in the formation of the designated compound, denoted as ^{99m}Tc-AgNPs-ICG.

3. HPLC analysis (high-performance liquid chromatography)

Nanoparticles suspension were analyzed by size-exclusion chromatographic high-performance liquid chromatography (SE-HPLC) was performed on a TSKgel G300SW XL 7.8 mm x 30 cm column (Tosoh Bioscience, LLC, Japan) eluted with double distilled water, at a flow rate of 1 mL/min; with an Agilent 1200 series equipment, with diode array detection NaI(Tl) scintillation detectors, sample injection volume of 25 μ L and detector UV $\lambda_1 = 420$ nm, $\lambda_2 = 254$ nm. Isocratic run time was 20 minutes.

4. Fluorescence imaging

One ml of AgNPs-ICG suspension was added to an Eppendorf tube and its fluorescence was measured in a *in vivo* MS FX PRO equipment (BRUKER Corporation). Analysis of the optical signal capture was performed using Bruker MI



Software. Fluorescence filters were as follows: ICG excitation = 760-785 and emission = 820-840. Fluorescence intensity for each of the probes was determined and reported as mean fluorescent intensity (MFI).

5. Particle size and IR Spectrum

AgNPs-ICG suspension size was determined in a Zetasizer equipment (DLS, Zetasizer Nano-ZS, Malvern Instruments). An AgNPs-ICG suspension was concentrated in nitrogen steam, and a sample of it was included in the sample-holder of an Agilent IR equipment with ATR module (Attenuated total reflectance Fourier transform infrared).

RESULTS

Silver nanoparticles, denoted as AgNPs-ICG, were synthesized in an aqueous milieu, employing a controlled temperature of 37° C with continuous agitation at 90 rpm. The solution's pH was calibrated to 6, laying the foundation for subsequent analyses. A UV-visible spectroscopic evaluation was conducted within the wavelength range of 200 to 700 nm, revealing an absorption peak at 408 nm, congruent with the characteristic plasmon absorption spectrum of these nanoparticles (19).

These parameters, along with the visual attributes of the suspension, underwent study over a duration of 7 days, affirming their stability without discernible alterations (Figure 1).

To ascertain the composition and characteristics of the AgNPs-ICG, we employed molecular exclusion chromatography via a PD10 column. The profiles of this analysis are depicted in Figure 2.

Intriguingly, the profiles distinctly reveal that the indocyanine green-loaded nanoparticles exhibit elution at an expedited rate, and their elution profile distinctly diverges from that of the free ICG. The nanoparticles were studied utilizing infrared spectrometry, revealing distinctive spectral bands at 3193, 2624, 1596, and 1212 cm^{-1} (Figure 3).

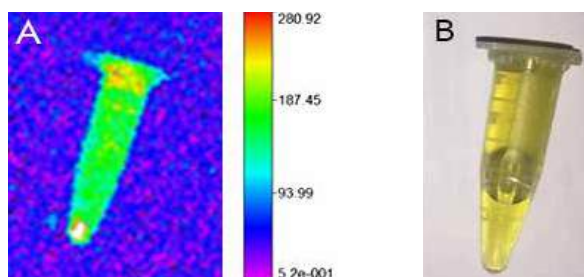


Figure 1A. Fluorescent image of AgNPs-ICG.

Figure 1B. Visible image of AgNPs-ICG.

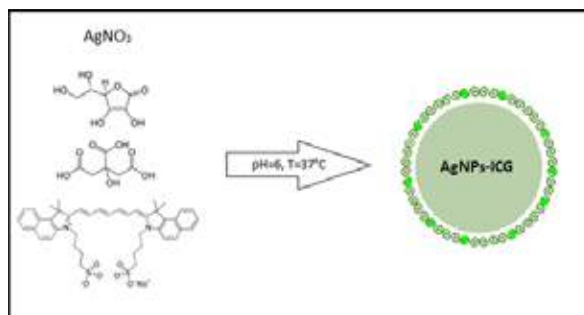


Figure 1C. Obtaining scheme of AgNPs-ICG.

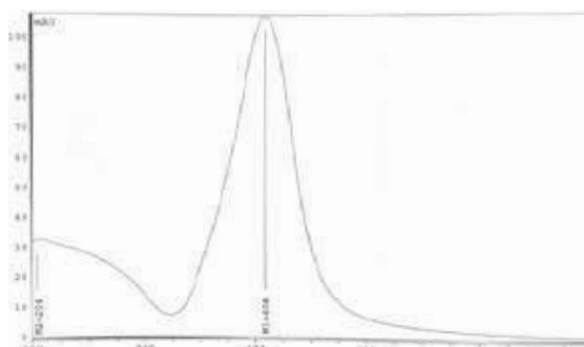


Figure 1D. UV visible spectrum of AgNPs-ICG.

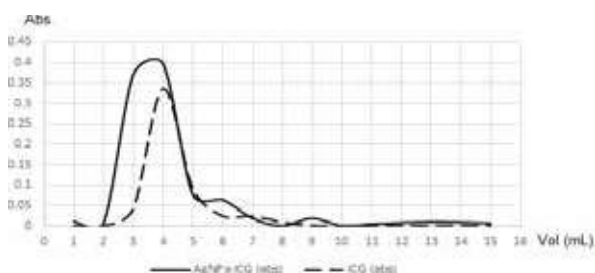


Figure 2. Size exclusion chromatography (PD-10).

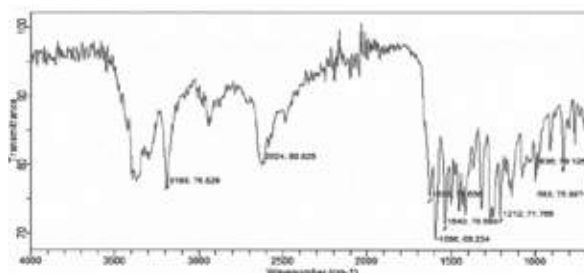


Figure 3. IR spectrum of AgNPs-ICG.

To elucidate their dimensional attributes, the AgNPs-ICG suspension's particle size was assessed employing laser light scattering equipment and singular-mode distribution was observed. This distribution presented a hydrodynamic diameter of 46.8 ± 1.7 nm, indicative of a well-defined and tightly regulated particle size, accompanied by a PDI value of 0.317 ± 0.041 (Figure 4).

The labelling process with ^{99m}Tc was successful, as the AgNPs-ICG nanoparticles were effectively loaded with ^{99m}Tc, resulting in the formation of ^{99m}Tc-AgNPs-ICG (Figure 5).

The radiochemical assessment of ^{99m}Tc-AgNPs-ICG nanoparticles via HPLC revealed a noteworthy concordance between the UV and gamma chromatograms, underscored by a confluence of retention times at the peak. This principal peak unveiled a distinct absorption band at 420 nm within its spectrum (Figure 6A).

Differentiating itself from pertechnetate, which exhibited a retention time of 11.6 minutes, the principal peak of the ^{99m}Tc-AgNPs-ICG nanoparticles demonstrated a distinct retention time of 7.2 minutes. This divergence in retention times serves as a robust indicator, indicating a radiochemical purity close to 100% (Figure 6B).

DISCUSSION

The different applications of metallic nanoparticles, particularly silver ones, have been studied since last decades. Specially, the development of radioactive-fluorescent hybrid agents is of great biomedical importance; they can be used for diagnosis and guide therapy in operating room through *in vivo* molecular imaging (20).

Ag NPs have emerged as promising nanomaterial-based radiosensitizers, enhancing the radiation-induced eradication of glioma cells, as demonstrated by Liu *et al.* in 2013 (21).

Treatment of cancer cells with Ag NPs exhibits dose-dependent cytotoxicity.

Smaller-sized NPs, such as 20 nm and 50 nm,

exhibit heightened cytotoxicity at relatively lower radiation doses. In hypoxic glioma cells, treatment with Ag NPs in combination with radiotherapy significantly augments anti-glioma effects, resulting in enhanced radiation efficacy. This effect may be attributed to increased apoptosis activity and robust autophagy induction (22).

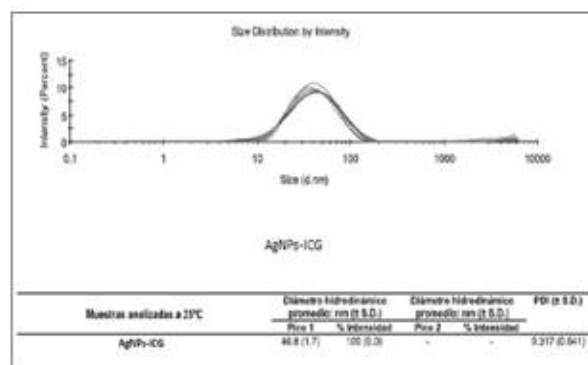


Figure 4. Particle size and IR spectra of AgNPs-ICG.

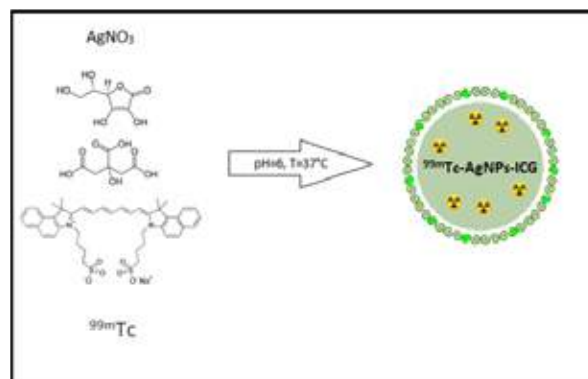


Figure 5. Labeling scheme of hybrid silver nanoparticles (^{99m}Tc-AgNPs-ICG).

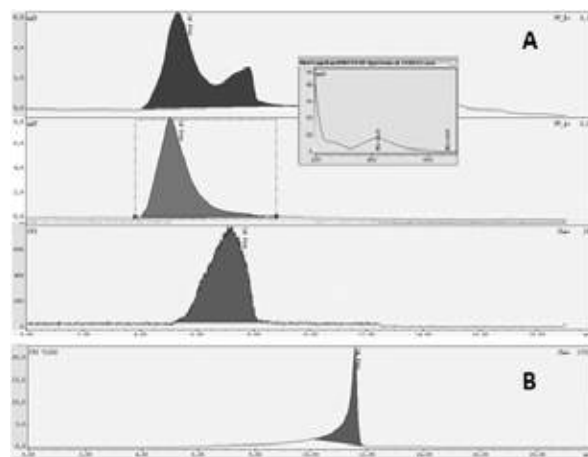


Figure 6A. HPLC perf of: ^{99m}Tc-AgNPs-ICG.

Figure 6B. HPLC perf of: Pertechnetate.



A recent study has shown promise by using modified Ag NPs coated with bovine serum albumin (BSA) and conjugated with verapamil (VRP). These modified Ag NPs have demonstrated effective accumulation in tumor cells, offering significant potential as high-efficiency nano radiosensitizers for glioma radiotherapy (23).

In the present study, we have synthesized and characterized fluorescent nanoparticles, denoted as AgNPs-ICG as potential theranostic agent. Fluorescent labelling is commonly used to monitor the biodistribution of nanomedicines. However, meaningful interpretation of the results requires that the fluorescent label remains attached to the nanomedicine. In this work, we explore the stability of AgNPs-ICG, wherein we assessed their size, and distribution. It was observed that these nanoparticles exhibited a uniform single-mode distribution, indicative of a highly controlled synthesis process. This consistency in size distribution is vital for their intended applications, particularly in the context of *in vivo* use, where uniformity can be crucial for ensuring consistent behavior and interactions within biological systems. Furthermore, an examination of the hydrodynamic diameter of the AgNPs-ICG was conducted, revealing a mean diameter of 46.8 ± 1.7 nm. This specific size range is a notable achievement, as it aligns well with the optimal dimension desirable for biomedical applications. Such dimensions have been associated with enhanced cellular uptake, prolonged circulation times, and minimized potential for clearance by the reticuloendothelial system, thereby highlighting the nanoparticles' suitability for *in vivo* use (24).

Fourier Transform Infrared Spectroscopy (FTIR) analysis show different stretches of bonds shown at different peaks; 2624—C—H; O—H, 1638—C=C, and 1212—C=O. Peaks near 3420 cm^{-1} and 2950 cm^{-1} assigned to OH stretching and aldehydic C—H stretching, respectively. The peak near 833 cm^{-1} assigned to C=CH₂. FTIR spectra of silver

nanoparticles exhibited prominent peaks at 2950 and 1638 cm^{-1} . The band 1370 developed for C—C stretching (25).

These observations collectively support the presence of silver nanoparticles and their interaction with organic ligands. These ligands likely engage with silver (Ag) through surface bonds formed between the most electronegative atoms and Ag's d orbitals. This interaction enables the aqueous stabilization of nanoparticles, yielding biocompatible attributes (26).

Moreover, our investigation extended to an assessment of the nanoparticles' stability over a period of 7 days, where the nanoparticles exhibited a remarkable stability profile, showcasing negligible alterations in their core properties. In addition to its primary function as a dye, ICG possesses the ability to convert light into heat and generate free radicals when activated by light (27).

These unique properties make ICG a promising candidate for serving as an effective photosensitizer in the context of photothermal therapy (PTT) for cancer treatment. It's worth noting that the cytotoxic effects of AgNPs are primarily observed at high concentrations, often in the range of several hundred micromolar concentrations (28).

To enhance their potential for cancer treatment, one effective approach is to load anti-cancer drugs or photosensitizers like ICG onto AgNPs. Furthermore, AgNPs serve as excellent nano carriers, particularly for heat-sensitive and water soluble compounds such as ICG. This advantage stems from the synthesis process of AgNPs, which doesn't necessitate the use of organic solvents or heating, making it highly favorable for these applications (29).

Taking our study further, we explore the dual labeled nanoparticles, namely ^{99m}Tc-AgNPs-ICG. This dual-labeling strategy, incorporating both radioactive and fluorescent moieties, holds immense potential for diverse applications

ranging from simultaneous imaging to targeted therapeutic interventions.

The HPLC-based analysis revealed that the dual-labeled nanoparticles exhibited a stable profile. The presence of both UV and GAMMA detectors enabled a comprehensive assessment of the nanoparticles' integrity, ensuring that both their fluorescent and radioactive components remained well-preserved over the course of the study.

The UV spectrum analysis unveiled a distinctive superficial plasmon resonance peak spanning the wavelength range of 400 to 450 nm, a hallmark feature that signifies the successful synthesis of silver nanoparticles (30).

We utilized HPLC with GAMMA detection to explore further. The resulting chromatogram revealed a unique peak, indicating the labeled nanoparticles (^{99m}Tc-AgNPs-ICG). This distinct peak differed significantly from the chromatogram of free Pertechnetate, confirming the specific presence of the labeled nanoparticles.

This differentiation highlights the successful integration of the radioactive label (^{99m}Tc) onto the AgNPs-ICG structure. The development of hybrid (fluorescent-radioactive) silver nanoparticles may open the path to novel diagnostic and therapeutic agents. Our study describes for the first time to our knowledge the development of silver hybrid (radioactive and fluorescent) nanoparticles. Their physiochemical properties were characterized being stable and their labelling was reproducible having potential biomedical applications.

CONCLUSIONS

In this study, we successfully synthesized silver nanoparticles (AgNPs) for the development of a hybrid imaging agent, ^{99m}Tc-AgNPs-ICG, with promising potential as a theranostic agent. We characterized the AgNPs-ICG nanoparticles through various techniques, including infrared spectrometry and laser light scattering, which

revealed a well-defined and tightly regulated particle size with a hydrodynamic diameter of 46.8 ± 1.7 nm and a low polydispersity index (PDI) value of 0.317 ± 0.041 . Subsequent loading of ^{99m}Tc onto the AgNPs-ICG nanoparticles was successful, resulting in the formation of ^{99m}Tc-AgNPs-ICG with nearly 100% radiochemical purity. The development of ^{99m}Tc-AgNPs-ICG opens exciting avenues for improved cancer diagnosis, treatment, and research, along with potential applications in various medical fields including: Image-Guided Surgery, Cancer Diagnosis and Treatment, Personalized Medicine and Treatment Response Monitoring.

Further research and clinical studies will be vital in realizing the full potential of this innovative theranostic agent.

CONFLICT OF INTEREST

The authors declare that they have no conflicts of interest. The study was carried out with the authors' own resources and/or those of the institution they represent.

REFERENCES

- (1) Burduşel AC, Gherasim O, Grumezescu AM, Mogoantă L, Fica A, *et al.* Applications of Silver Nanoparticles: An Up-to-Date Overview. *Nanomaterials (Basel)* 2018 Sep; 8(9):681. DOI: 10.3390/nano8090681.
- (2) Clement JL, Jarrett PS. Antibacterial Silver. *Met Based Drugs* 1994; 1(5-6):467-482. DOI: 10.1155/MBD.1994.467.
- (3) Saji VS, Choe HC, Young KW. Nanotechnology in biomedical applications—a review. *Int J Nano Biomater* 2010; 3:119-139. DOI: 10.1504/IJNB.2010.037801.
- (4) Heiligtag FJ, Niederberger M. The fascinating world of nanoparticle research. *Mater Today* 2013; 16:262-271. DOI: 10.1016/j.mattod.2013.07.004.



- (5) Syafiuddin A, Salmiati Salim MR, Kueh ABH, Hadibarata T, Nur H. A Review of silver nanoparticles: Research trends, global consumption, synthesis, properties, and future Challenges. *J Clin Chem Soc* 2017; 64:732-756. DOI: 10.1002/jccs.201700067.
- (6) Zhang XF, Liu ZG, Shen W, Gurunathan S. Silver Nanoparticles: Synthesis, Characterization, Properties, Applications, and Therapeutic Approaches. *Int J Mol Sci* 2016 Sep 13; 17(9):piiE1534. DOI: 10.3390/ijms17091534.
- (7) Rao CNR, Müller A, Cheetham AK. Nanomaterials – An Introduction. Cap. 1, p.1-11. <https://doi.org/10.1002/352760247X.ch1>. Sastry M. Moving Nanoparticles Around: Phase-Transfer Processes in Nanomaterials Synthesis. Cap. 3, p.31-50. <https://doi.org/10.1002/352760247X.ch3>. In: Rao CNR, Müller A, Cheetham AK (Eds.). *The Chemistry of Nanomaterials. Synthesis, Properties and Applications* Weinheim : Wiley-VCH Verlag GmbH & Co. KGaA, 2004.
- (8) Ouay BL, Stellacci F. Antibacterial activity of silver nanoparticles: A surface science insight. *Nano Today* 2015; 10:339-354. DOI: 10.1016/j.nantod.2015.04.002.
- (9) Mie G. Beiträge zur Optik trüber Medien, speziell kolloidaler Metallösungen. *Annalen der Physik* 1908; 330(3):377-445. DOI: 10.1002/andp.19083300302.
- (10) Zhang XF, Liu ZG, Shen W, Gurunathan S. Silver nanoparticles: Synthesis, characterization, properties, applications, and therapeutic approaches. *Int J Mol Sci* 2016; 17:1534. DOI: 10.3390/ijms17091534.
- (11) Ghosh R, Girigoswami K. NADH dehydrogenase subunits are overexpressed in cells exposed repeatedly to H₂O₂. *Mutat Res* 2008; 638(1-2):210-215. DOI: 10.1016/j.mrfmmm.2007.08.008
- (12) Asharani PV, Hande MP, Valiyaveetil S. Anti-proliferative activity of silver nanoparticles. *BMC Cell Biol* 2009; 10:65. Published 2009 Sep 17. DOI: 10.1186/1471-2121-10-65.
- (13) Hsin YH, Chen CF, Huang S, Shih TS, Lai PS, Chueh PJ. The apoptotic effect of nanosilver is mediated by a ROS- and JNK-dependent mechanism involving the mitochondrial pathway in NIH3T3 cells [published correction appears in *Toxicol Lett* 2008 Mar 10; 185(2):142]. *Toxicol Lett* 2008; 179(3):130-139. DOI: 10.1016/j.toxlet.2008.04.015.
- (14) Sanpui P, Chattopadhyay A, Ghosh SS. Induction of apoptosis in cancer cells at low silver nanoparticle concentrations using chitosan nanocarrier. *ACS Appl Mater Interfaces* 2011; 3(2):218-228. DOI: 10.1021/am100840c.
- (15) Ahamed M, Karns M, Goodson M, Rowe J, Hussain SM, Schlager JJ, *et al.* DNA damage response to different surface chemistry of silver nanoparticles in mammalian cells. *Toxicol Appl Pharmacol* 2008; 233(3):404-410. DOI: 10.1016/j.taap.2008.09.015.
- (16) Sukirtha R, Priyanka KM, Antony JJ, Kamalakkannan S, Thangam R, Gunasekaran P, *et al.* Cytotoxic effect of green synthesized silver nanoparticles using *Melia azedarach* against in vitro HeLa cell lines and lymphoma mice model. *Process Biochem* 2012; 47:273-279. DOI: 10.1016/j.procbio.2011.11.003.
- (17) Chen D, Dougherty CA, Yang D, Wu H, Hong H. Radioactive Nanomaterials for Multimodality Imaging. *Tomography* 2016 Mar; 2(1):3-16. DOI: 10.18383/j.tom.2016.00121.
- (18) Gambini JP, Silvera E, Musetti M, Quinn T, Zhong Yang G, Matalonga S, *et al.* ^{99m}Tc nanocolloid indocyanine green: An hybrid tracer for breast sentinel node procedures. *J Nucl Med* 2019 May 1; (60)supplement 1:1231.

- (19) Ider M, Abderrafi K, Eddahbi A, Ouaskit S, Kassiba A. Silver Metallic Nanoparticles with Surface Plasmon Resonance: Synthesis and Characterizations. *J Clust Sci* 2017; 28:1051-1069. DOI: 10.1007/s10876-016-1080-1.
- (20) Herrmann K, Nieweg OE, Povoski SP (Eds.). Radioguided surgery. Current Applications and Innovative Directions in Clinical Practice. Switzerland: Springer International, 2016.
- (21) Liu P, Huang Z, Chen Z, Xu R, Wu H, Zang F, *et al.* Silver nanoparticles: a novel radiation sensitizer for glioma? *Nanoscale* 2013; 5(23):11829-11836. DOI: 10.1039/c3nr01351k.
- (22) Liu Z, Tan H, Zhang X, Zhou Z, Hu X, Zhang H, *et al.* Enhancement of radiotherapy efficacy by silver nanoparticles in hypoxic glioma cells. *Artif Cells Nanomed Biotechnol* 2018; 46(sup3):S922-S930. DOI: 10.1080/21691401.2018.1518912.
- (23) Zhao J, Li D, Ma J, Yang H, Chen W, Cao Y, *et al.* Increasing the accumulation of aptamer AS1411 and verapamil conjugated silver nanoparticles in tumor cells to enhance the radiosensitivity of glioma. *Nanotechnology* 2021; 32(14):145102. DOI: 10.1088/1361-6528/abd20a.
- (24) Lee SH, Jun BH. Silver Nanoparticles: Synthesis and Application for Nanomedicine. *Int J Mol Sci* 2019 Feb 17; 20(4):865. DOI: 10.3390/ijms20040865.
- (25) Marimuthu S, Rahuman AA, Rajakumar G, Santhoshkumar T, Kirthi AV, Jayaseelan C, *et al.* Evaluation of green synthesized silver nanoparticles against parasites. *Parasitology Research* 2011; 108(6):1541-1549. DOI: 10.1007/s00436-010-2212-4.
- (26) Frost MS, Dempsey MJ, Whitehead DE. The response of citrate functionalised gold and silver nanoparticles to the addition of heavy metal ions. *Colloids and Surfaces A: Physicochemical and Engineering Aspects* 2017 Apr 5; 518:15-24. DOI: 10.1016/j.colsurfa.2016.12.036.
- (27) Sheng Z, Hu D, Xue M, He M, Gong P, Cai L. Indocyanine Green Nanoparticles for Theranostic Applications. *Nano-Micro Lett* 2013; 5:145-150. DOI: 10.1007/BF03353743.
- (28) Ding J, Chen G, Chen G, Guo M. One-Pot Synthesis of Epirubicin-Capped Silver Nanoparticles and Their Anticancer Activity against Hep G2 Cells. *Pharmaceutics* 2019 Mar 15; 11(3):123. DOI: 10.3390/pharmaceutics11030123.
- (29) De Matteis V, Cascione M, Toma CC, Leporatti S. Silver Nanoparticles: Synthetic Routes, In Vitro Toxicity and Theranostic Applications for Cancer Disease. *Nanomaterials (Basel)* 2018 May 10; 8(5):319. DOI: 10.3390/nano8050319.
- (30) Gonzalez AL, Noguezn C, Beranek J, Barnard AS. Size, Shape, Stability, and Color of Plasmonic Silver Nanoparticles. *J Phys Chem C* 2014; 118:9128-9136. DOI: 10.1021/jp5018168.

CONTRIBUTIONS TO THE MANUSCRIPT:

- (a) Conception; design; data acquisition; data analysis; interpretation and discussion of results; drafting and critical revision; and approval of the final version.
- (b) Design; Data Acquisition.
- (c) Design; Data Acquisition.
- (d) Data analysis; interpretation and discussion of results; drafting and critical revision.
- (e) Data analysis; interpretation and discussion of results; drafting and critical revision.
- (f) Design; data analysis; interpretation and discussion of results; critical writing and review.
- (g) Data analysis; interpretation and discussion of results; critical writing and review.
- (h) Conception; design; data analysis; interpretation and discussion of results; drafting and critical revision; and approval of the final version.

NOTE: This article was approved by the Editorial Committee.